Electron spin resonance of a Co^{2+} pair in $Mg_{1-x}Co_xCl_2$ coupled by anisotropic exchange interactions

1989 J. Phys.: Condens. Matter 1 10507

(http://iopscience.iop.org/0953-8984/1/51/020)

J. Phys.: Condens. Matter **1** (1989) 10507–10514. Printed in the UK

Electron spin resonance of a Co^{2+} pair in $Mg_{1-x}Co_xCl_2$ coupled by anisotropic exchange interactions

K Katsumata† and J Tuchendler‡

† The Institute of Physical and Chemical Research (RIKEN), Wako, Saitama 351-01, Japan

‡ Laboratoire de Dispositifs Infrarouge, Université Paris VI, 4 Place Jussieu, 75230 Paris Cedex 05, France

Received 1 August 1989

Abstract. Electron spin resonance (ESR) experiments at millimeter and submillimeter wavelengths performed on single crystals of the randomly diluted system $Mg_{1-x}Co_xCl_2$ with the low x-values are reported. A set of novel ESR lines has been observed near the paramagnetic line. We assign these lines as arising from Co^{2+} ions pairs coupled by anisotropic exchange interactions. A good agreement between the theory and the experiment is attained.

1. Introduction

The compounds $CoCl_2$ and $MgCl_2$ have the same hexagonal (rhombohedral) $CdCl_2$ structure. The lattice parameters differ only slightly. Moreover, the melting points of the two compounds are almost the same. Thus, we expect that $CoCl_2$ and $MgCl_2$ will make good solid solutions over the entire range of concentration. Cobalt dichloride orders antiferromagnetically at 24.9 K [1]. The ordered-state spin structure is such that spins within a metal layer form a ferromagnetic sheet and the spins in adjacent layers are antiparallel [2]. The spins are confined into the c-plane and the anisotropy within the plane is very small. The ground state of Co^{2+} in $CoCl_2$ is a doublet [3, 4]. The first excited state lies about 200 cm^{-1} above it [1]. Then, one may use an effective spin $s = \frac{1}{2}$ to describe the magnetic properties of $CoCl_2$ at low temperatures. The isotropic exchange interactions between the true Co^{2+} spins ($S = \frac{3}{2}$) become anisotropic when they are truncated to the $s = \frac{1}{2}$ system. Also, the g-value becomes anisotropic in the $s = \frac{1}{2}$ system. There is no single ion anisotropy (DS_z^2) for $s = \frac{1}{2}$ spin and the magnetic dipole–dipole interaction between the Co^{2+} moments is much weaker than the anisotropic exchange interactions. So, the main origin of the anisotropy of Co^{2+} spin in $CoCl_2$ comes from the anisotropic exchange interactions. Since the electronic state of Co^{2+} depends on its ligand, we expect that the ground-state properties of $CoCl_2$, such as the g-values and the anisotropic exchange interactions, will not change significantly with dilution by $MgCl_2$.

In an earlier paper [5] we reported that we were able to follow the way in which the antiferromagnetic resonance modes in $CoCl_2$ change with dilution. We were able to analyse the results using the theory with anisotropic exchange interactions [6]. In this paper we report the results of electron spin resonance (ESR) experiments performed on $Mg_{1-x}Co_xCl_2$ with Co^{2+} concentrations much lower than the percolation concentration

0953-8984/89/5110507 + 08 $02.50

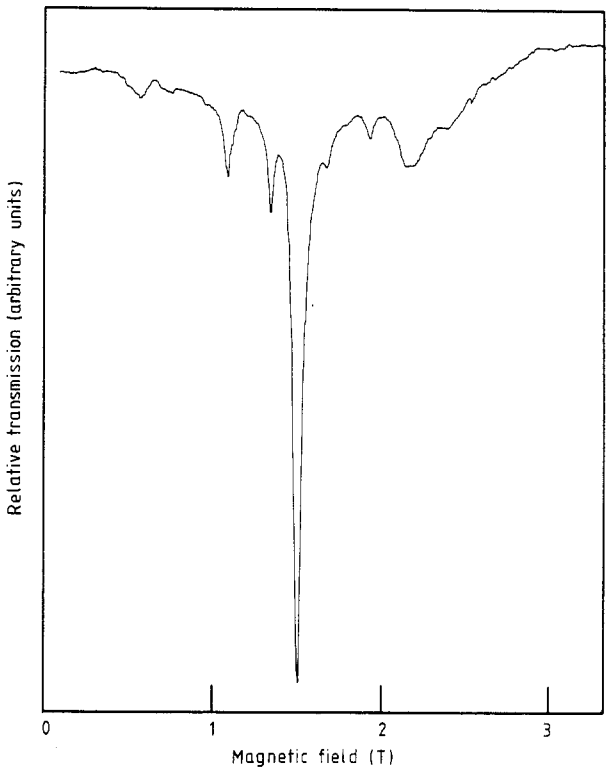

Figure 1. A typical example of the recorder traces of ESR signals obtained in the $x = 0.093$ single crystal at $T = 4.2$ K. The intensity of the microwave at 60 GHz transmitted through the sample is recorded against the external magnetic field: $j \| H_0$.

($x_c \cong 0.3$). We have observed many ESR lines. As described below, we have succeeded in explaining these ESR lines; they come from a Co^{2+} pair coupled by anisotropic exchange interactions. Cobalt pair spectra in $CdCl_2$-type compounds have been observed in the infrared [7] and far-infrared [8] regions. These experiments were performed in zero external magnetic field with spectral resolution poorer than that of ESR. Consequently, only a few lines could be observed.

The single crystals of $Mg_{1-x}Co_xCl_2$ were prepared in the same way as was reported earlier [5]. The cobalt and magnesium concentrations of the actual samples used in the experiment were determined by means of induced coupled plasma-atomic emission spectrometry. The set up of the ESR experiment has been described in detail previously [9].

2. Experimental results

We show in figure 1 a typical example of the recorder traces of ESR signals obtained in the $x = 0.093$ sample. The external magnetic field (H_0) is parallel to the crystalline c axis. We see a sharp and intense central line and weaker satellite lines. The resonance fields at various frequencies observed in the $x = 0.093$ sample with $H_0 \| c$ are plotted in

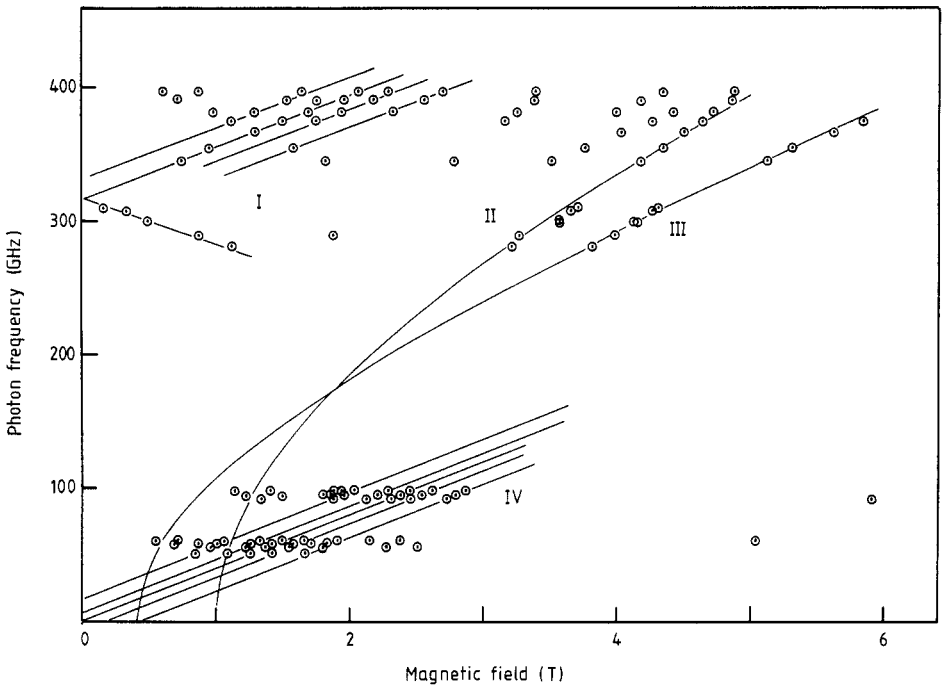

Figure 2. Frequency–field dependences of the resonance line positions obtained in the $x = 0.093$ sample of at $T = 4.2$ K for the external magnetic field parallel to the c-axis ($H_0 \| c$). The full lines are the theoretical ones discussed in the text.

figure 2. We have obtained essentially the same results in a crystal sample with $x = 0.054$. Figure 3 shows a typical example of the recorder traces of ESR signals observed in the $x = 0.093$ sample for $\boldsymbol{H}_0$ perpendicular to the c axis. Three strong and many weaker lines are seen. We have plotted in figure 4 the frequency–field relations of the ESR signals obtained in the $x = 0.093$ sample with $H_0 \perp c$. The result for the crystal with $x = 0.055$ is essentially the same.

3. Analysis

The frequency–field relations of the ESR signals labelled II, IV and V in figure 4 are described following the theory developed in [5]. In a similar way, we can calculate the frequency–field relations of the resonance modes when $\boldsymbol{H}_0$ is rotated by 90° from the c-plane. A detail of the calculation will be reported elsewhere. The fit of the experimental points is shown in figure 2 where the lines II and III are theoretical ones. The resonance modes labelled I in figures 2 and 4 are the same as those observed in the $x = 0.21$ sample [10]. Subsequently, we confine ourselves in this paper to the ESR modes IV shown in figure 2 and VI in figure 4. The hyperfine interaction between the electron and nuclear spins of Co^{2+} [11] is too weak to explain the splittings between the ESR lines. Therefore one has to look for another origin of the splitting.

In the following, we calculate the ESR frequencies of Co^{2+} pair coupled by an anisotropic exchange interaction.

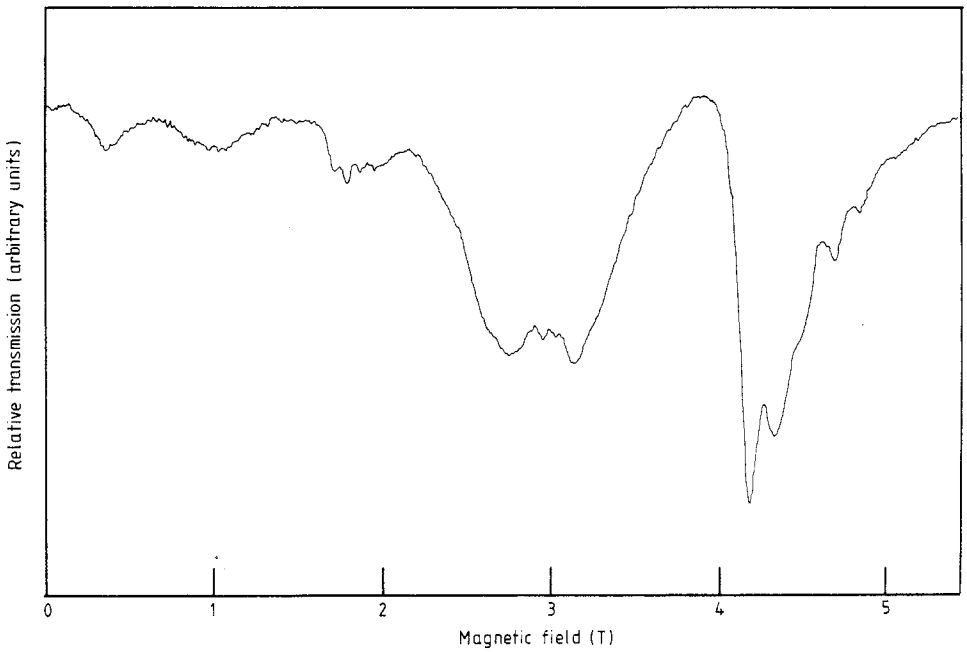

Figure 3. A typical example of the recorder traces of ESR spectrum obtained at 291 GHz in the $x = 0.093$ single crystal at $T = 4.2$ K. The external field is applied in the c-plane ($H_0 \perp c$).

3.1. External magnetic field parallel to the c axis

Taking the quantisation axis (z) parallel to $\boldsymbol{H}_0$, the Hamiltonian may be written as,

$$\mathcal{H} = -2j(s_1^x s_2^x + s_1^y s_2^y) - 2Js_1^z s_2^z + g_\parallel \mu_B H_0 (s_1^z + s_2^z) \tag{1}$$

where, s_1 and s_2 are the spin operators ($=\frac{1}{2}$) of Co^{2+} at sites 1 and 2, j and J the components of the exchange constant in the $xy(c)$-plane and along the $z(c)$-axis respectively, $g_\parallel$ the g-value along the c-axis, and μ_B the Bohr magneton. The fact that Co^{2+} spins of $CoCl_2$ lie in the c-plane means $|J| < |j|$. The states of the pair system are constructed from all possible combinations of $|s_1^z = \pm\frac{1}{2}, s_2^z = \pm\frac{1}{2}\rangle$. The eigenvalues of the Hamiltonian are easily obtained by solving the secular equation. The energies are

$$E = -J/2 \pm g_\parallel \mu_B H_0 \qquad \text{and} \qquad E = J/2 \pm j. \tag{2}$$

Since the matrix representation of equation (1) with respect to the above four states has off-diagonal elements, we expect many allowed transitions between the energy levels given by equation (2). The ESR frequencies (ν) are given by

$$\begin{cases} h\nu = j + J \pm g_\parallel \mu_B H_0 & (3a) \\ h\nu = j - J \pm g_\parallel \mu_B H_0 & (3b) \\ h\nu = -j - J + g_\parallel \mu_B H_0 & (3c) \\ h\nu = -j + J + g_\parallel \mu_B H_0 & (3d) \\ h\nu = 2g_\parallel \mu_B H_0 & (3e) \end{cases}$$

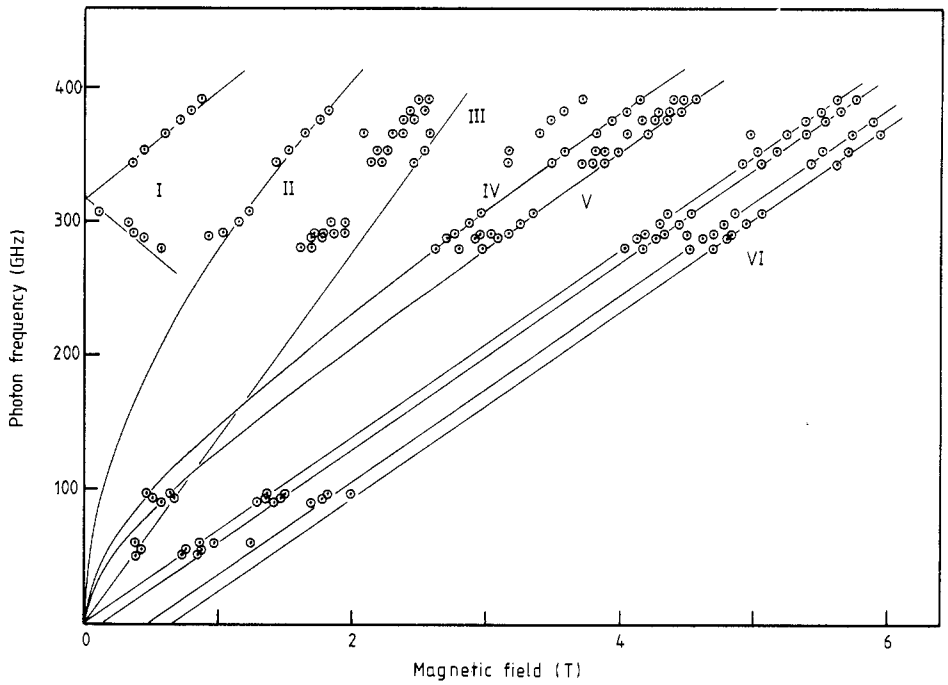

Figure 4. Frequency against magnetic field relations of the ESR signals observed in the $x = 0.093$ sample at $T = 4.2$ K for the external field applied in the c-plane ($H_0 \perp c$). The full lines labelled I to V are the theoretical ones discussed in the text, while the lines VI are drawn only as a guide to eye.

where h is Planck's constant. An interesting feature of the ESR caused by the Co^{2+} pair coupled by anisotropic exchange interaction is the appearance of the new lines expressed by $h\nu = j - J \pm g_{\parallel}\mu_B H_0$ and $h\nu = -j + J + g_{\parallel}\mu_B H_0$. In the isotropic case, these lines merge into the paramagnetic line.

Now, we compare theory with experiment. In the mode IV of figure 2 we see five straight lines through the experimental points. These lines are parallel to each other and the spacings are different, as the theory predicts. From the slope of these lines we obtain the g-value. The spacings give the exchange constants. By fitting the experiment with equation (3), we get the following values;

$$g_{\parallel} = 2.81 \qquad |j| = 0.37\ \text{cm}^{-1} \qquad |J| = 0.17\ \text{cm}^{-1}. \tag{4}$$

The ESR line with equation (3e) has not been observed in this configuration.

3.2. *External magnetic field perpendicular to the c axis*

We take the quantisation axis (z) parallel to $\boldsymbol{H}_0$ in the c-plane and the y axis along the crystalline c axis. Then, the Hamiltonian may be written as

$$\mathcal{H} = -2Js_1^y s_2^y - 2j(s_1^x s_2^x + s_1^z s_2^z) + g_{\perp}\mu_B H_0(s_1^z + s_2^z) \tag{5}$$

where $g_{\perp}$ is the g-value in the c-plane. The eigenvalues of the Hamiltonian are

$$E = j + J/2 \qquad E = -J/2 \qquad E = -j/2 \pm [(J-j)^2 + 4g_{\perp}^2\mu_B^2 H_0^2]^{1/2}/2. \tag{6}$$

From equation (4), the value of $(j - J)$ is $0.20\ \text{cm}^{-1}$, which corresponds to the Zeeman

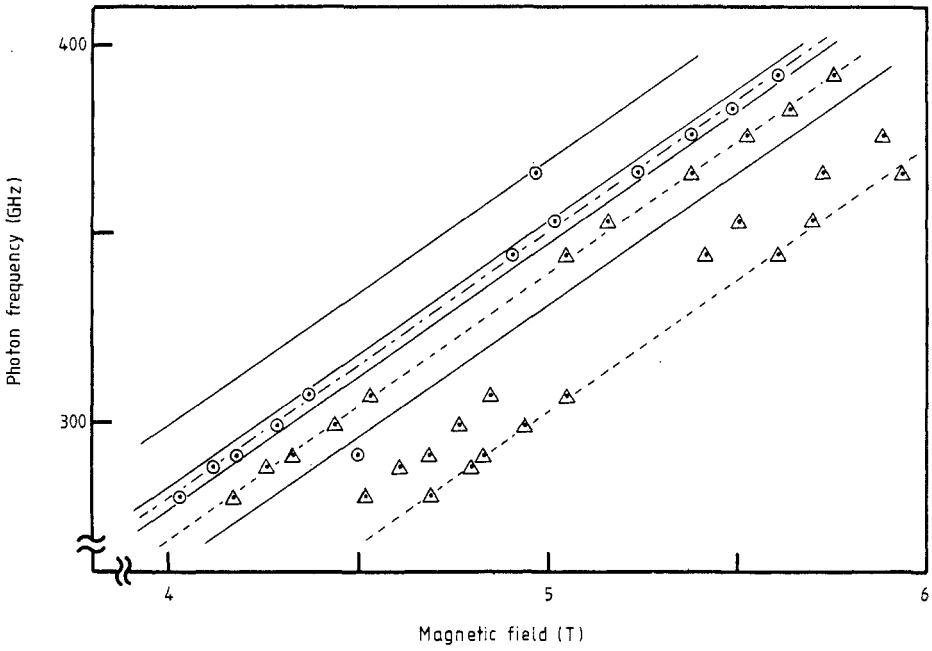

Figure 5. The experimental data of the mode VI in figure 4 at the high frequency and high field region are compared with the result of the present calculation. The full and dotted lines are the theoretical ones. The dot-dashed line is the paramagnetic line. $T = 4.2$ K, $H_0 \perp c$.

energy of about 0.1 T ($g_\perp = 5.00$ is used, as in references [5, 10]). Because the ESR signals of the mode VI in figure 4 are observed above about 0.7 T, we may neglect the $(J - j)^2$ term of equation (6) in analysing the data. Then, the ESR frequencies are given by

$$\begin{cases} h\nu = 3j/2 + J/2 \pm g_\perp \mu_B H_0 & (7a) \\ h\nu = j/2 - J/2 + g_\perp \mu_B H_0 & (7b) \\ h\nu = -j/2 + J/2 + g_\perp \mu_B H_0 & (7c) \\ h\nu = -3j/2 - J/2 + g_\perp \mu_B H_0 & (7d) \\ h\nu = 2g_\perp \mu_B H_0. & (7e) \end{cases}$$

We compare now theory with experiment. From the slope of the lines VI in figure 4, we get the value 5.00 for $g_\perp$. Using the exchange constants determined before (equation (4)), we draw as full curves in figure 5 the result of the calculation. The experimental points lie on these lines. However, there are many experimental points (the triangles in figure 5) that do not belong to the theoretical lines. In order to analyse these experimental data, we introduce another set of exchange constants. The dotted curves in figure 5 are the theoretical ones with $|j'| = 0.98$ cm^{-1} and $|J'| = 0.25$ cm^{-1}. The ESR signal with twice the g-value in equation (7*e*) has been observed in this configuration (mode III in figure 4).

3.3. Discussion on the exchange constants

In this section, we discuss the exchange constants obtained from the present study. Lines [4] has studied theoretically the magnetic properties of $CoCl_2$. He considered the exchange Hamiltonian

$$\mathcal{H}_{1m} = Js_1 \cdot s_m - Ds_1^{x'} s_m^{x'}, \tag{8}$$

where x' is taken parallel to the c axis. By fitting the theory with available experimental information, Lines determined the following values

$$\begin{aligned} &D/J = 0.425 \qquad J_1 = -14.5\ \text{cm}^{-1} \qquad D_1 = -6.13\ \text{cm}^{-1} \\ &J_2 = 1.24\ \text{cm}^{-1} \qquad D_2 = 0.53\ \text{cm}^{-1} \end{aligned} \tag{9}$$

where J_1 and J_2 are the exchange constants in the c-plane and between the planes, respectively. The experimental values determined by Hutchings [1] from the neutron scattering study are

$$\begin{aligned} &J_1 + J_3 = -19.8\ \text{cm}^{-1} \qquad D_1 + D_3 = -11.1\ \text{cm}^{-1} \\ &J_2 = 1.50\ \text{cm}^{-1} \qquad D_2 = 2.29\ \text{cm}^{-1} \end{aligned} \tag{10}$$

where J_3 is the next-nearest-neighbour exchange constant in the c-plane. From these values we have the ratios, $(D_1 + D_3)/(J_1 + J_3) = 0.561$ and $D_2/J_2 = 1.53$. The former is consistent with the result of Lines (equation (9)), while the latter is largely different from the theoretical value. In order to compare our results with those by Lines and Hutchings, the following conversions of the exchange parameters should be made; J(Lines) $\rightarrow -2j$(ours), $(J - D)$(Lines) $\rightarrow -2J$(ours). Since the present experiment does not give any information on the signs of the exchange constants, we discuss only their absolute values. The exchange parameter (j) determined in this study (equation (4)) is smaller than any of those obtained by Lines and Hutchings. On the other hand, the ratio $(j - J)/j$ that corresponds to D/J in the Hamiltonian of Lines is 0.54. This value is close to that of $(D_1 + D_3)/(J_1 + J_3)$ determined from the neutron scattering experiment [1]. Then, it can be said that the j interaction in equation (1) comes from a further neighbour in the c-plane.

Next, we discuss the j' interaction. We have obtained the value 0.98 cm^{-1} for j' from the present experiment, which should be read as 1.96 cm^{-1} in the Hamiltonians of Lines and Hutchings. This value is not so different from that of J_2 determined from the neutron scattering experiment (equation (10)). Thus, we assign the ESR lines to the ones from the Co^{2+} pair coupled with the between-planes exchange interaction. The ratio $(j' - J')/j'$ is 0.74 from our experiment, which lies in between the theoretical value (0.425) and the experimental one (1.53) determined from the neutron scattering study.

Acknowledgments

We would like to thank Mrs S Kawai for her help in growing the single crystals of $Mg_{1-x}Co_xCl_2$ and Dr Y Takahashi for the chemical analysis. One of the present authors (KK) would like to thank the members of the Laboratoire de Dispositifs Infrarouge, Université Paris VI for their warm hospitality. This work was partially supported by a Research Fund from RIKEN and by a Grant-in-Aid for Scientific Research from the Japanese Ministry of Education, Science and Culture.

References

[1] Hutchings M T 1973 *J. Phys. C: Solid State Phys.* **6** 3143
[2] Wilkinson M K, Cable J W, Wollan E O and Koehler W C 1959 *Phys. Rev.* **113** 497
[3] Kanamori J 1958 *Prog. Theor. Phys.* **20** 890
[4] Lines M E 1963 *Phys. Rev.* **131** 546
[5] Katsumata K, Kawai S and Tuchendler J 1988 *Solid State Commun.* **65** 1211
[6] Date M 1961 *J. Phys. Soc. Japan* **16** 1337
[7] Johnstone I W and Jones G D 1977 *Phys. Rev.* B **15** 1297
[8] Wiltshire M C K 1979 *J. Phys. C: Solid State Phys.* **12** 3571
[9] Tuchendler J, Magariño J and Renard J P 1979 *Phys. Rev.* B **20** 2637
[10] Katsumata K, Kawai S and Tuchendler J 1988 *J. Physique Coll.* **49** C8 1091
[11] Morigaki K 1961 *J. Phys. Soc. Japan* **16** 1639